

# Online High-Speed PMSM Parameters Estimation and Stability Analysis

Martin Novák<sup>1</sup>, Aymen Flah<sup>2</sup>, Jaroslav Novák<sup>3</sup>, Sbita Lassaad<sup>4</sup>

<sup>1,3</sup>Czech Technical University in Prague, Faculty of Mechanical Engineering, Department of Instrumentation and Control Engineering, Technická 4, 166 07 Prague, Czech republic, martin.novak@fs.cvut.cz, jaroslav.novak@fs.cvut.cz

<sup>2,4</sup>National school of engineering of Gabes, University of Gabes, Zrig, Gabes 6029, Tunisia, flah.aymen@hctl.org, lassaad.sbita@enig.rnu.tn

---

*Abstract: This paper presents a solution for identifying the variance of high-speed Permanent Magnet Synchronous Motor (PMSM) parameters in different states. The proposed method is based on the Model Reference Adaptive System (MRAS) and implements vector control. Flux weakening is used to ensure the functionality of the machine above the nominal speed (25,000 RPM) up to the maximal speed 42,000 RPM. The estimation method allows fast online parameter estimation. The estimated parameters have been verified experimentally, and the obtained results are in good agreement with other identification methods. Specific issues in modeling of high-speed machines are also addressed in the paper and a novel approach to closed loop PMSM control system stability analysis is proposed.*

*Keywords: Computational modeling; Experimental verification; High-speed motors; Permanent magnet motors; MRAS; time-delay system; stability*

---

## 1 Nomenclature

$v_d, v_q$  – voltage in d,q axes [V]

$R_s$  – stator resistance [ $\Omega$ ]

$\lambda_m$  – flux linkage [Wb]

$i_d, i_q$  – currents in d,q axes [A]

$L_d, L_q$  – inductance in d,q axes [H]

$\omega$  – electrical speed [rad/s]

$J$  – moment of inertia [ $\text{kgm}^2$ ]

$F$  – friction damping coefficient [N/rad/s]

$K_{air\_fric}$  – air friction damping coefficient [N/rad<sup>2</sup>/s<sup>2</sup>]

$p_p$  - number of pole-pairs [-]

$\tau$  - time constant [s]

$Td$  - time delay [s]

$H(s)$  - transfer function

## 2 Introduction

Recently the area of high-speed machines has seen a lot of development. In particular, high-speed applications using permanent magnet synchronous motors (PMSM) promise very interesting results. This is due to their high power density: small volume and weight for high output power. The power density of high-speed machines is in the range 0.2-0.6 [kg/kW]. For “the normal speed” PMSM the power density is around 1 [kg/kW]. A comparison of 3 high-speed machines and their parameters is shown in Table 1. A more detailed comparison is shown in [1]. Whether or not the machine requires cooling depends on its required usage, and this is indicated in the table. It is clear that although high-speed PMSMs promise advantages such as small volume and weight per unit of power, they also present significant challenges. The main challenge is selecting suitable bearings for the machine. Although viable options such as high speed ceramic ball bearings, magnetic bearings and so on exist, they are very expensive. Another challenge is the control of high-speed motors. The traditional approach for controlling high-speed PMSM is the V/f control method [2]-[9]. In order to achieve high control over the system dynamics, field-oriented control (FOC) is preferable. However, FOC for a high-speed machine requires hardware with a high speed digital signal processor (DSP) or a field-programmable gate array (FPGA) such as in [8], [10].

It was shown in [13] [14], that the production of such a high-speed machine is possible. The PMSM motor developed here has the rated velocity 240,000 RPM, and a rated output power equal to 5 kW. Even so, the motor dimensions were small with stator and rotor diameter 60 mm and 20 mm respectively. Such high efficiency applications are needed in the industry, as shown in [9]. Also, high-speed machines are becoming of interest to the energy production industry due to the development of microturbine generators, combined heat and power units etc. [15].

Generally, when a high speed operation is required, the flux weakening method is used [16]. The currents are controlled in such a way as to create a magnetic field acting against the permanent magnet flux in order to limit back-emf. This changes not only the flux linkage, but other machine parameters as well. The change in PMSM parameters will, in turn, have an influence on the control quality, and eventually the system stability.

Therefore, identifying parameter variations in the system is preferable. The controller setting can then be determined by known experimental or simulation methods.

For simulation experiments a motor model is required. Although modeling of PMSM's is generally well known [17]-[20], some specific issues of high-speed machines that are neglected for low speeds have to be considered in their high-speed counterparts.

Table 1  
Power density of different machines

Type	PMSM1	PMSM2	PMSM3
Power (kW)	0.1/0.2 without/with cooling	3	2
Weight (kg)	0.038	1.4	1.3/2.4 (with cooling)
Power density (kg/kW)	0.38/0.19	0.47	0.65/1.2
Nominal speed (RPM)	500k	240k	200k
Application	Celerotron CM-2-500 [11]	Micro-Combined Heat and Power, MTT, Eindhoven	[12]

These issues will be addressed in the course of this paper, together with the experimentally determined PMSM parameter identification. Also, comparison of experimental and simulated results will be discussed.

It is further known that PMSM parameters are not constant: they change with temperature, frequency, load etc. The whole system is nonlinear, and the change of parameters can also have a significant impact on stability [21]. Therefore, the purpose of this paper is to provide a novel online identification method for estimating the variance of PMSM parameters during motor operations. In addition, time delay in the system can cause system instability. Therefore, a novel method based on analysis of the time delay system is also proposed.

### 3 PMSM Model

The PMSM model is based on the electrical properties of the stator windings and on their interaction with the rotor. The described model was developed in [22], wherein its experimental verification was also completed. Therefore, the used model will be described only briefly. The novelty in the herein proposed model lies in the consideration of air friction in the motor. This is an important loss in a high-speed machine as it can be even greater than bearing losses [23].

State space model of PMSM is

$$\frac{dX}{dt} = A \cdot X + B \cdot U + N_1 \cdot X \cdot \omega + X^T \cdot N_2 \cdot X \quad (1)$$

Where,

$$\frac{dX}{dt} = \begin{bmatrix} \frac{di_d}{dt} \\ \frac{di_q}{dt} \\ \frac{d\omega}{dt} \end{bmatrix} \quad X = \begin{bmatrix} i_d \\ i_q \\ \omega \end{bmatrix} \quad U = \begin{bmatrix} v_d \\ v_q \\ T_L \end{bmatrix} \quad (2)$$

$$A = \begin{bmatrix} \frac{-R_s}{L_d} & 0 & 0 \\ 0 & \frac{-R_s}{L_q} & \frac{-\lambda_m}{L_q} \\ 0 & \frac{3 p_p^2}{2 J} \lambda_m & \frac{-p_p F}{J} \end{bmatrix} \quad B = \begin{bmatrix} \frac{1}{L_d} & 0 & 0 \\ 0 & \frac{1}{L_q} & 0 \\ 0 & 0 & \frac{-p_p}{J} \end{bmatrix} \quad (3)$$

$$N_1 = \begin{bmatrix} 0 & \frac{L_q}{L_d} & 0 \\ \frac{-L_d}{L_q} & 0 & 0 \\ 0 & 0 & 0 \end{bmatrix} \quad N_2 = \begin{bmatrix} 0 & \frac{3 p_p^2}{2 J} (L_d - L_q) & 0 \\ 0 & 0 & 0 \\ 0 & 0 & -\frac{p_p K_{air\_fric}}{J} \end{bmatrix} \quad (4)$$

The PMSM model based on (2) - (4), together with the equation for torque was used to create a model of the system, and to identify and verify it with the experimental results obtained from the real system.

## 4 Real PMSM Model Parameter Identification

To set the PMSM model correctly it was necessary to estimate some model parameters. Some of these could be determined directly from the manufacturer's data in Table 2, while others required additional experiments.

Table 2  
Motor data

Motor type: 2AML406B-090-10-170
Manufacturer: VUES Brno, CZ
$V_{dc} = 560$ V
$I_{n,rms} = 11$ A
$T_n = 1.2$ Nm
$n_n = 25\,000$ min <sup>-1</sup> , $n_{max} = 42\,000$ min <sup>-1</sup>
$K_E = 7.3$ V/kRPM

To estimate other electrical and mechanical motor parameters two different methods were used and the results compared. Method one consisted of a direct measurement with a LCRG Meter Tesla BM591, where both winding resistance and inductance were measured. In method two, resistance was measured with Ohm's method using a Diametral Q130R50D power supply and 2x Pro's kit digital multi-meters, MT1232. The inductance was calculated from the time constant of a transient characteristic using oscilloscope GDS-806C, with probe GTP-060A. For nominal current, the inductance was 1.1 mH. The motor's moment of inertia was calculated from a motor startup shown in Figure 1. In this experiment the motor was powered with a given current  $I_q = 9$  A, until flux weakening started. The start time was 0.4 s and the reached frequency was 572 Hz (speed 34 320 min<sup>-1</sup>). The startup current, 9 A, corresponds to torque 0.98 Nm. Considering the relatively high current and torque, mechanical losses were neglected in the calculations. Detailed results are available in [22]. The final identified model parameters are summarized in Table 3.

As can be seen from the model, air friction losses are considered. This is important for high-speed machines as the losses caused by air friction can be as high as friction losses in bearings. According to [23], where the speed was 500,000 RPM, friction losses caused by air friction were 8 W, whereas bearing losses were 10 W for two bearings (i.e. 5 W for one bearing).

As the machine used for this research has maximal speed 42,000 RPM, it can be expected that air friction losses will be much lower. In the herein presented model, air friction losses are still considered as a custom machine design to obtain 250,000 RPM is currently under development. In this machine, the air friction component may be quite significant.

The friction torque is a function of  $\omega^2$ . An experiment was made to estimate bearing and air friction. It consists of accelerating the motor to its maximum speed and turning off the inverter. The rotor will slow down naturally. The deceleration of the rotor is measured as a function of time.

Table 3  
PMSM model parameters

Model parameter	Value and units	note
$R_s$	210 [mΩ]	Average from direct and indirect measurement
$L_d = L_q$	1100 [μH]	1100 (for I = I <sub>n</sub> = 11 A)
$\Psi_m$	0.072 [Wb]	
$J$	$0.11 \cdot 10^{-3}$ [kgm <sup>2</sup> ]	
$F$	$8.2 \cdot 10^{-5}$ [N/rad/s]	
$K_{air\_fric}$	$1.3 \cdot 10^{-10}$ [N/rad <sup>2</sup> /s <sup>2</sup> ]	Very small, could be significant for higher speeds

It is obvious that when the motor is un-powered and unloaded, its mechanical speed will decrease due to the losses until a still stand. This is described by the following dynamic equation

$$\frac{d\omega}{dt} = -\frac{p_p F}{J} \omega - \frac{p_p K_{air\_fric}}{J} \omega^2 \quad (5)$$

It has to be noted that (5) does not represent all losses in the motor.

The solution of (5) is given by

$$\omega(t) = \frac{F \cdot \omega(0)}{F \cdot e^{\left(\frac{F \cdot t}{J}\right)} - K_{air\_fric} \cdot \omega(0) + K_{air\_fric} \cdot \omega(0) \cdot e^{\left(\frac{F \cdot t}{J}\right)}} \quad (6)$$

Equation (6) was used to find coefficients  $F$  and  $K_{air\_fric}$  from experimentally measured PMSM rotor deceleration. The search was made using the method of least squares in Matlab.

The comparison in Figure 2 is the best match that could be achieved simply by changing parameters  $F$  and  $K_{air\_fric}$ . As can be seen, there are some significant differences, especially for lower speeds. This is because other losses in the motor have been neglected, one such is the loss caused by eddy currents. As the permanent magnet is rotating, it induces currents to the stator windings and stator iron. There is also an interaction between the permanent magnet and those currents. Stator core losses could be determined by the Steinmetz equation [24] [25]. However, the herein described differences are not an issue for this application, as only high speeds are anticipated.

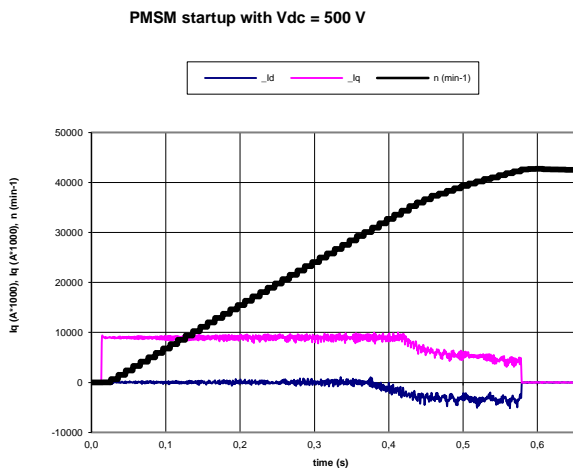


Figure 1  
PMSM startup to speed 42 000 RPM

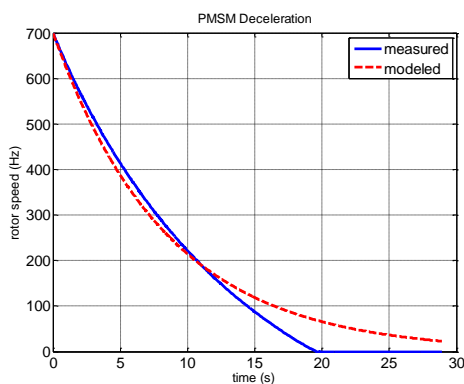


Figure 2  
Simulation and experimental results comparison for PMSM spin-down

Another loss that has been neglected is reluctance loss - the interaction between the permanent magnet and stator iron. In other words, the permanent magnet is attracted to the stator iron, which then produces a braking force on it. This is visible when the rotor is turned by a bare hand. It can also be seen that the rotor takes preferably one of four positions. This effect seems to be significant for lower rotor speeds. Considering these simplifications, the presented fit can be considered as an approximate model. However, as the model was designed for high-speed application only this is considered sufficient.

In order to verify the parameter values and their changes during various machine states, an online PMSM parameter estimator is developed in the following chapter.

## 5 Online PMSM Parameters Identification

In this part the Model Reference Adaptive System (MRAS) estimator is developed to identify PMSM parameters variations online. The proposed estimator needs only the online measurement of current, voltage, and rotor speed in order to simultaneously estimate the stator resistance, inductance and the rotor flux linkage.

By choosing  $d$  and  $q$  stator current components as state variables, the PMSM state system takes the form of equation (7) and the adjustable parameter state system can be expressed in equation (8):

$$\dot{X} = AX + BU + C \quad (7)$$

Where  $A = \begin{bmatrix} -\tau & \omega \\ -\omega & -\tau \end{bmatrix}$ ;  $B = \begin{bmatrix} c & 0 \\ 0 & c \end{bmatrix}$ ;  $C = \begin{bmatrix} 0 \\ -e_f \end{bmatrix}$ ; the current state vector is:  $X = [i_d \ i_q]^T$

, the command vector is  $U = [v_d \ v_q]^T$  and

$$c = \frac{1}{L_s} \quad \frac{1}{\tau} = \frac{L_s}{R_s} \quad e_f = \omega I_f \quad I_f = \frac{\lambda_m}{L_s}$$

$$\dot{\hat{X}} = \hat{A}\hat{X} + \hat{B}U + \hat{C} + G(\hat{X} - X) \quad (8)$$

Where  $\hat{A} = \begin{bmatrix} -\hat{\tau} & \hat{\omega} \\ -\hat{\omega} & -\hat{\tau} \end{bmatrix}$ ;  $\hat{B} = \begin{bmatrix} \hat{c} & 0 \\ 0 & \hat{c} \end{bmatrix}$ ;  $\hat{C} = \begin{bmatrix} 0 \\ \omega \hat{I}_f \end{bmatrix}$  and  $G = \begin{bmatrix} k_1 & 0 \\ 0 & k_2 \end{bmatrix}$

$G$  represents the correction gain matrix to be chosen so as to achieve pre-specified error characteristics, where  $k_1, k_2$  are two limited positive real, manually adjusted numbers. By subtracting the adjustable parameter system, equation (8), from the state system (7), the error function system can be defined in equation (9):

$$\dot{e} = \Delta A e + \Delta B U + \Delta C + G e \quad (9)$$

The nonlinear time variable feedback system, which includes a feed forward linear model and a nonlinear feedback system is:

$$\dot{e} = \underbrace{(A + G)e}_{\text{feed forward linear model}} + \underbrace{\left( -\Delta A \hat{X} - \Delta B U - \Delta C \right)}_{\text{Nonlinear feedback system}} \quad (10)$$

The study of the system stability can be resolved with the POPOV stability theory. Two necessary conditions must be satisfied as demonstrated in [26] and [16]:



- The transfer function matrix of the linear forward block must be real and strictly positive. According to [16] the gain matrix  $G$  shown in equation (9) guaranties this condition.
- The nonlinear feedback block must meet the POPOV integral inequality presented as:  $\int_0^{t_1} w^T edt \geq -\gamma^2$ , where  $\gamma^2$  is a positive constant for any time  $t$ .

By decomposing the second POPOV condition, three new conditions are obtained and expressed in (11).

$$\left\{ \begin{array}{l} \int_0^{t_1} e^T (\hat{A} - A) \hat{X} dt \geq -\gamma_A^2 \\ \int_0^{t_1} e^T (\hat{B} - B) U dt \geq -\gamma_B^2 \\ \int_0^{t_1} e^T (\hat{C} - C) dt \geq -\gamma_C^2 \end{array} \right. \quad (11)$$

Conditions (11) are satisfied if the adaptive algorithm is designed in a similar way to a PI controller. This is shown in the following equations:

$$\left\{ \begin{array}{l} \Delta A = \int_0^t (e^T \hat{X} \cdot f_{ir} + e^T \hat{X} \cdot f_{pr}) dt \\ \Delta B = \int_0^t (e^T U \cdot f_{il} + e^T U \cdot f_{pl}) dt \\ \Delta C = \int_0^t (e^T \cdot f_{ic} + e^T \cdot f_{pc}) dt \end{array} \right. \quad (12)$$

The adaptive parameters expressions are:

$$\left\{ \begin{array}{l} \frac{\hat{R}_s}{\hat{L}_s} = -\left(k_{pr} + \frac{k_{ir}}{s}\right) \left(\hat{i}_d e_d + \hat{i}_q e_q\right) + \frac{\hat{R}_s}{\hat{L}_s} (0) \\ \frac{1}{\hat{L}_s} = \left(k_{pl} + \frac{k_{il}}{s}\right) \left(v_d e_d + v_q e_q\right) + \frac{1}{\hat{L}_s} (0) \\ \frac{\hat{\lambda}_m}{\hat{L}_s} = -\left(k_{pf} + \frac{k_{if}}{s}\right) \left(\omega e_q\right) + \frac{\hat{\lambda}_m}{\hat{L}_s} (0) \end{array} \right. \quad (13)$$

The global structure of the adaptive algorithm parameters identification is shown in Figure 3.

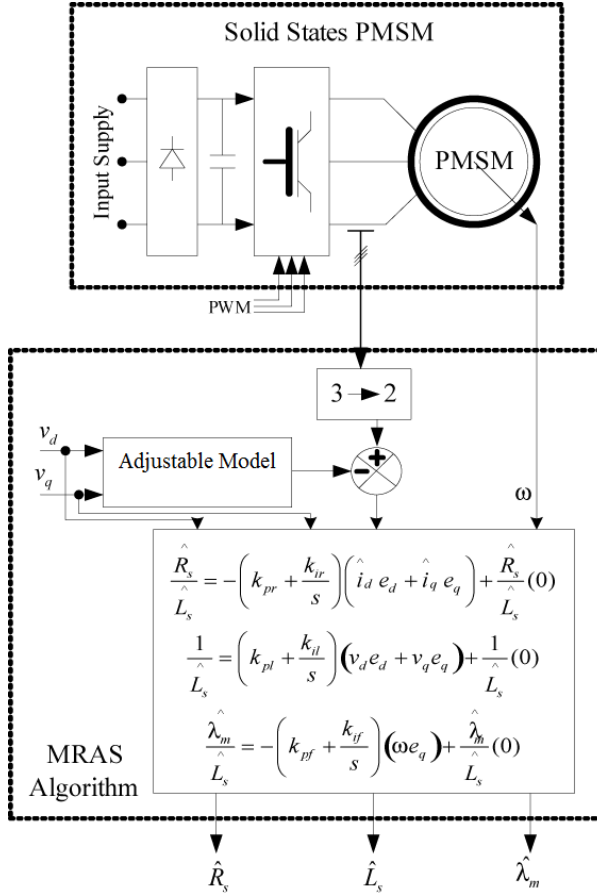


Figure 3

Online MRAS-PMSM parameters identification scheme

## 6 Description of the Experimental System

The experimental setup is shown in Figure 4. The power network voltage is rectified to DC voltage. The DC voltage supplies an insulated gate bipolar transistor (IGBT) inverter built for this purpose. The inverter is using power module SKM75GD124D and an IGBT/MOSFET driver SKHI61 both from Semikron. The whole system is being prepared to work as a microturbine generator; the turbine is created by means of a standard automotive turbocharger.

This has the advantages of: good availability, high reliability and low price. For the purpose of system testing, the turbocharger is connected to a compressed air

supply; and in the future a combustion chamber will be built. Some other alternatives for the turbine have also been considered like a model aircraft turbine or a real aerospace turbine.

Currently, the machine is used as a motor i.e. providing mechanical energy to the turbocharger. When a suitable source of compressed air or exhaust gas is available, it will be run in generator mode to produce electrical energy

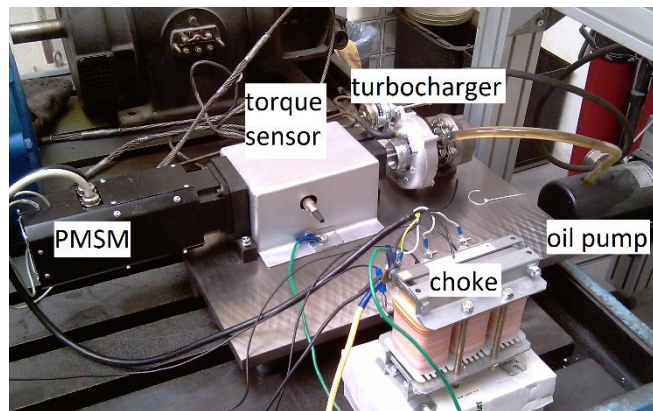


Figure 4  
Experimental setup

## 7 Estimation Results

Figure 5 shows the overall PMSM control and identification scheme. The oriented vector control is used as the motor control strategy, where three PI controllers are implemented to control the currents and the speed. The flux weakening block is used to generate the reference direct stator current.

The MRAS block is used for the online estimation of the PMSM parameters variation. Only stator currents and voltages are needed to ensure this operation.

Two experiments are shown. Figure 6 demonstrates a simple start and stop of the machine, while Figure 7 shows the machine response to variations of current  $I_q$ ; this corresponds to different torques and speeds. The current for this experiment was adjusted manually. The three upper sub-charts in both figures show PMSM angular velocity  $\omega$ ,  $i_d$  and  $i_q$  currents respectively. This was used as input to the MRAS estimator. The requested  $I_d$  current was set to 0 A in both cases. Current  $I_q$  was set to 2 A in the experiment shown in figure 6, and adjusted manually in the second experiment, depicted in figure 7, to achieve the required speed profile. The lower three sub-charts represent the output from the estimator and show the changes of  $R_s$ ,  $L_s$  and  $\lambda_m$  respectively. Firstly, the experiment shown in Figure 6 is

analyzed. As can be seen from the estimated value of  $R_s$ , there is a relatively large variation. The estimated value for standstill is 210 m $\Omega$ . This value was also obtained by other methods, as described in Table 3. For maximal speed 42,000 RPM (corresponds to angular speed 700 Hz in the chart),  $R_s$  changes to 250 m $\Omega$ . The relative change is about 20%. As the experiment took only a short time, the variations are not expected to be caused by the change of temperature. Moreover,  $R_s$  drops back to the initial value as soon as the motor slows down. A clear dependence between angular velocity  $\omega$  and  $R_s$  can be found. For this particular PMSM,  $R_s$  increases by about 3% per 100 Hz of  $\omega$ . The same effect can also be observed in Figure 7, where a more complex speed profile is shown. The initial overshoot is believed to be caused by the settling properties of the estimator, as this acts like a PI controller. The behavior of machine inductance,  $L_s$ , is different. After the initial undershoot, there is a visible increase in inductance in the first case, but a decrease in the second case. As the changes between the initial and instantaneous value of  $L_s$  are quite small, no conclusions can be made here. However, the initial value of  $L_s$  has been estimated correctly and corresponds to the measured value of inductance. The permanent magnet magnetic flux,  $\lambda_m$ , shows a decrease in both experiments. Nevertheless, this decrease is very small and, although it was confirmed during all other experiments, it was not possible to draw a clear quantitative conclusion, like it was for the case of  $R_s$ , due to the expected accuracy of the experiments. However, the initial value of  $\lambda_m$  has been again correctly estimated.

The effect of the varying load has not been tested. It would require significant changes in the test setup and a different kind of load. Moreover a when the herein described tests were finished, the PMSM – turbocharger coupling encountered a mechanical failure at it was necessary to redesign the experimental setup.

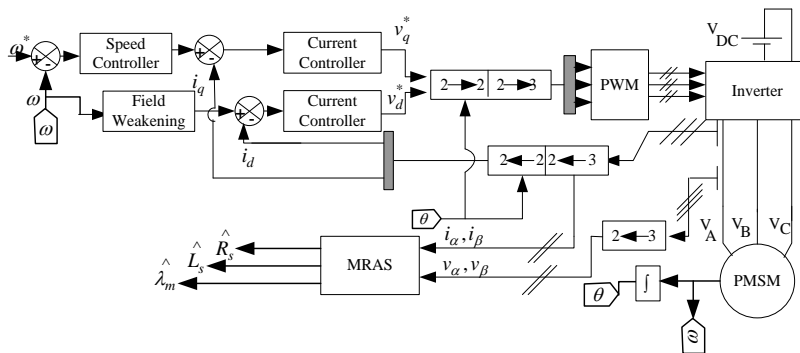


Figure 5

Block diagram of the PMSM control and parameters identification

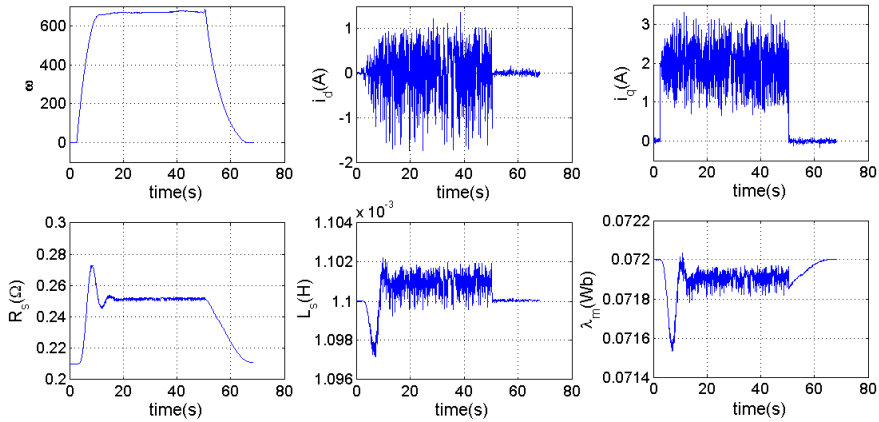


Figure 6

PMSM model parameters change for startup and spin-down

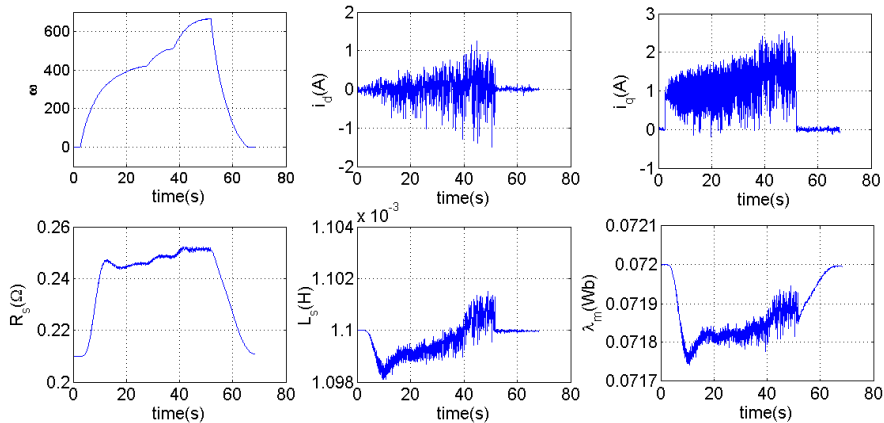


Figure 7

PMSM model parameters change for a startup with requested torque change

## 8 Stability Analysis

The stability of PMSM is an important issue. Although it may not seem so, the machine itself can become unstable due to the variance of machine parameters with temperature, current, load and even applied frequency from the inverter. By “frequency”, the fundamental current harmonics—variable with speed—are meant here. There are two possible approaches to address the stability analysis.

The first one is to analyze the inherent stability of the machine itself, i.e. to look at its properties in an open loop—from the perspective of the machine designer. High speed PMSM's are usually not equipped with damper windings due to space or losses constraints [21] [27]. Many high-speed PMSM's are used only in V/f control mode. This is suitable for applications with predictive and known load, such as fans or compressors. When the inverter applies frequency exceeding a certain range, the machine can become unstable [28]. Because both the inductance and resistance of the PMSM vary significantly with frequency, a significant margin in the motor stability is required [29].

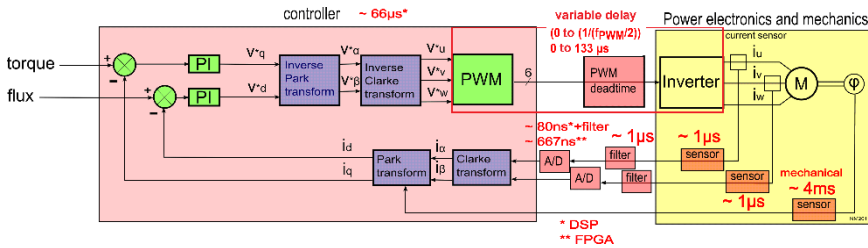


Figure 8

Control system block diagram with an estimate of time delays—adapted from [10]

The mechanical analogy of the magnetic field in a PMSM could be a spring and a dampener. When too much torque is applied (from the stator field), or when the frequency is too high, the rotor permanent magnet is not able to follow the stator field and the stator-rotor linkage breaks. This is equivalent to applying too much force on the mechanical spring. An analysis for this open loop V/f approach has been done in [30]. Although in this case it was an axial flux PMSM, it shows that stability analysis can be very important right from the start of machine design.

The second possibility to analyze stability is to look at the PMSM and the controller together, and to analyze the closed loop system using FOC. The main advantage of FOC is the ability to achieve higher machine dynamics, and the possibility to control the machine torque precisely. On the other hand, this requires a significant amount of computational power available in the FOC controller. Due to the small stator resistance and inductance, the electrical time constant of the machine is small. In the case of the herein described PMSM it is 5.2 ms. The mechanical time constant of the motor is about 250x higher, in this case 1.3 s. As the mechanical time constant is significantly higher than the electrical time constant, the mechanical speed is usually considered to be constant in the analysis [31].

It was shown in [30], [32] that the electrical time constant can be as small as 26  $\mu$ s. This means the delay added by multiple sources in the system can be significant. Sources such as: anti-aliasing filter, A/D converter, PI controller algorithm, inverter dead-time etc. The final system is one that exhibits time delay, and without proper precautions it can be very difficult to control and stabilise. It is

therefore important for high-speed machine control systems to estimate the influence of delays on system stability.

An estimate of the time delays in the analyzed system is shown in figure 8. Two cases are shown. The first one (marked \*) is for a DSP controller system, the second one (marked with \*\*) is for an FPGA system, currently under development. From the values of time delays, some important features can be predicted. There are two significant time delays. One is in the controller itself. It is caused by the fact that it takes some time for the algorithm to calculate the new values of controller outputs. This delay is fixed, it is 66  $\mu\text{s}$  for the DSP system used in this application. The second dominant time delay is caused in the PWM and in the inverter itself. Moreover, this delay is variable, in the case of our system it is from 0 to 133  $\mu\text{s}$  depending on where the controller action update "hits" the PWM triangular signal.

The other time delays are relatively insignificant compared to those two. The fact that the time delay is high and that it is variable, leads to possible stability issues when higher speeds are required, or if the machine parameters are changing. The stability analysis of a system can be done by analyzing pole placement. A time delay system, with time delay,  $T_d$ , is described with a transfer function in general form as:

$$H(s) = e^{-s \cdot T_d} \quad (14)$$

The problem of stability analysis—in finding the roots—of (14) is that the number of roots is infinite. The solution adopted in this paper uses the approach described in [34]-[36]. It is an algorithm able to find roots in a selected area of the complex plane. Using this algorithm, a simulation of the system was done with variable time delay from 0 to 300  $\mu\text{s}$ . The results are shown in Figure 9.

The upper part represents the selected area where the roots have been calculated, the bottom part is a close-up view of the values around the origin. Several important conclusions can be made from this analysis. Firstly and most importantly, the system becomes unstable for time delay above 270  $\mu\text{s}$ . The poles of the system have positive real parts of the roots and the system will be unstable no matter how sophisticated the control algorithm is. Considering the fixed time delay of the controller (66  $\mu\text{s}$ ) and the variable time delay (0 to 133  $\mu\text{s}$ ), the stability margin is quite low, only about 70  $\mu\text{s}$  in the worst case. The variability of time delay will also cause changing properties of the system in time.

These time delay changes will be, more or less, random depending on where the control variable update "hits" the PWM triangular signal. It can be seen that for this application, the time delay can't be higher than 270  $\mu\text{s}$ . This represents about 1/20th of the electrical time constant (5.2 ms). From this analysis, it is clear that a high-speed PMSM, when regarded as a whole, i.e. together with a controller, has to be considered as a time-delay system.

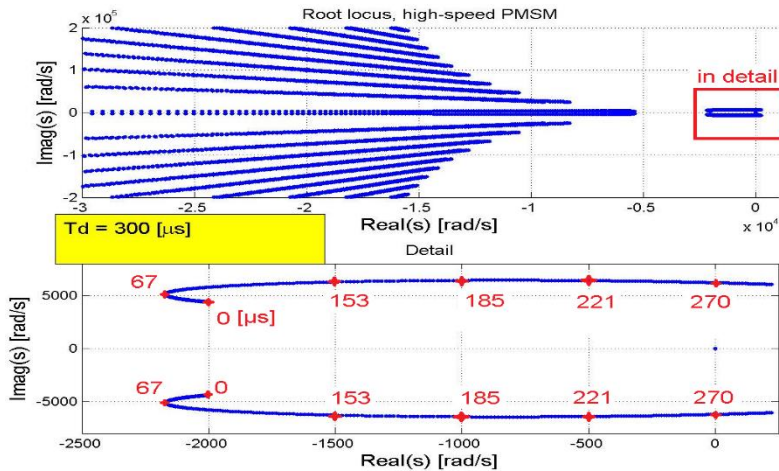


Figure 9

Root locus of PMSM - Controller model with time delay - detail around origin

## Conclusions

This paper presented a novel online MRAS estimator able to estimate changes in PMSM parameter variations during different states of the machine. It is shown that for the tested machine, there is a significant change in stator winding resistance,  $R_s$ , as the motor speed increases. This variation represents about a 20% increase in comparison with the initial value of  $R_s$ . As the experiments took only a short time, this change is not believed to be caused by the temperature variations. Changes in the stator winding inductance,  $L_s$ , and permanent magnet magnetic flux,  $\lambda_m$ , have also been observed, but due to their small change, no quantitative conclusions could have been made for  $L_s$  and  $\lambda_m$ .

A novel method for the analysis of the system as a whole, and as a time delay system, has been proposed. It is shown that for the presented machine, the time delay can't be higher than about 1/20th of the system time constant to maintain stability. An open question remains. How, and if, for the tested machine are the parameters changing with the load? As the PMSM was tested with only a constant load this could not have been tested. Modifications of the test setup are being prepared in order to allow changes to the load in the future to investigate this.

## Acknowledgement

This work was supported in part by the internal CTU Grant SGS12/178/OHK2/3T/12 "Development of measuring, simulation and experimental methods with focus on nontraditional energy source" and grant TE01020020 "Josef Bozek Competence Centre for Automotive Industry".

## References



- 
- [1] Novak, M.: Stability Issues of Electromechanical Systems with High-Speed Permanent Magnet Machines, Habilitation Thesis, Czech Technical University in Prague, 2012
- [2] Zhao, L. – Ham, Ch. H. – Wu, T. X – Zheng, L. – Seigneur, H.P. – Sundaram, B. – Kapat, J. – Vaidya, J. – Chow, L.: Development of A Super High-Speed Permanent Magnet Synchronous Motor (PMSM) Controller and Analysis of The Experimental Results, In: Journal of Systemics, Cybernetics and Informatics, Volume 3 - Number 1, ISSN 1690-4524
- [3] Zwysig, C. – Duerr, M. – Kolar, J.W.: An Ultra-High-Speed, 500000 rpm, 1 kW Electrical Drive System, In: Proceedings of Power Conversion Conference - Nagoya, 2007. PCC '07, Nagoya, Japan, ISBN 1-4244-0844-X, DOI: 10.1109/PCCON.2007.373174
- [4] Ko, J-S. – Kim, H. - Yang S-H.: Precision Speed Control of PMSM Using Neural Network Disturbance Observer on Forced Nominal Plant, In: Proceedings of Control Conference, 2004. 5<sup>th</sup> Asian 08/2004; 3:1746- 1752 Vol. 3
- [5] Bae, B-H. – Sul, S-K. – Kwon, J-H. - Shin J-S: Implementation of Sensorless Vector Control for Super-High Speed PMSM of Turbo-Compressor, In: IEEE Transactions on Industry Applications, Volume : 39(3), pp. 811-818, 05/2003
- [6] Zwysig, C. – Kolar, J. W. – Thaler, W. – Vohrer, M.: Design of a 100 W, 500000 rpm Permanent Magnet Generator for Mesoscale Gas Turbines, In: Proceedings of Industry Applications Conference, 2005. Fourtieth IAS Annual Meeting. Conference Record of the 2005, pp. 253-260, Vol. 1, ISBN 0-7803-9208-6, DOI 10.1109/IAS.2005.1518318
- [7] Zhao, L. – Ham, Ch. H. – Han, Q. – Wu, T. X. – Zheng, L. – Sundaram, K. B. – Kapat, J. – Chow, L.: Design of An Optimal V/f Control for a Super High Speed Permanent Magnet Synchronous Motor, In: Proceedings of 30<sup>th</sup> Annual Conference of the IEEE Industrial Electronics Society, November 2004, Busan, Korea, ISBN 0-7803-8730-9, DOI: 10.1109/IECON.2004.1432151
- [8] Kennel, R.: Ultra High Speed Drive with Permanent Magnet Synchronous Motors and Hardware Based Field Oriented Control, In.: Proceedings of the Electrical Machines and Power Electronics conference, 2007, ACEMP '07. International Aegean Conference on, pp. 116-124, ISBN 978-1-4244-0890-0, DOI: 10.1109/ACEMP.2007.4510493
- [9] Rahman, M. A. – Chiba, A. – Fukao, T.: Super High Speed Electrical Machines - Summary, In: Extended Summary for IEEE-PES Meeting at Denver 2004 Panel Session on Super High Speed Drive, ISBN 0-7803-8465-2, DOI: 10.1109/PES.2004.1373062

- 
- [10] Novak, M.: Research Setup for Special Purpose Permanent Magnet Synchronous Machines, Habilitation thesis, Czech Technical University in Prague, Faculty of Mechanical Engineering, 2012
- [11] Permanent-magnet machine CM-2-500, Celerotron Datasheet, Available on <<http://www.celerotron.com/datasheets/en/Datasheet-CM-2-500.pdf>>, [accessed 26.9.2012]
- [12] Pfister, P-D. - Perriard, Y.: Very-High-Speed Slotless Permanent-Magnet Motors: Analytical Modeling, Optimization, Design, and Torque Measurement Methods, In: IEEE Transactions on Industrial Electronics, Vol. 57, No. 1, January 2010
- [13] Oyama, J. – Higuchi, T. – Abe, T. – Shigematsu, K. – Yang, X. – Matsuo, E.: A Trial Production of a Small Size Ultra-High Speed Drive System, In: Proceedings of the Electric Machines and Drives Conference, 2003, IEMDC'03. IEEE International, pp. 31-36, Vol. 1, ISBN 0-7803-7817-2, DOI: 10.1109/IEMDC.2003.1211239
- [14] Oyama, J. – Higuchi, T. – Abe, T. – Shigematsu K. – Moriguchi R.: The Development of Small Size Ultra-High Speed Drive System, In: Proceedings of the Power Conversion Conference - Nagoya, 2007, PCC '07, pp. 1571-1576, ISBN 1-4244-0844-X, DOI: 10.1109/PCCON.2007.373173
- [15] Anh, J. B. – Jeong, Y. H. – Kang, D. H. – Park, J. H.: Development of High Speed PMSM for Distributed Generation Using Microturbine, In: Proceedings of 30<sup>th</sup> Annual Conference of the IEEE Industrial Electronics Society, November 2004, Busan, Korea, ISBN 0-7803-8730-9, DOI: 10.1109/IECON.2004.1432151
- [16] Flah A. - Sbita L. - Ben H. M. "Online MRAS-PSO PMSM Parameters Estimation", In: International Review of Modeling and Simulation IREMOS, Vol. 4, No. 3, pp. 980-987, 2011
- [17] Quang, N. P. – Dittrich, J. A.: Vector Control of Three-Phase AC Machines, Springer, 2008, ISBN 978-3540790280
- [18] Zhang, Z. – Shu, J.: Matlab-based Permanent Magnet Synchronous Motor Vector Control Simulation, In: Proceedings of the Computer Science and Information Technology (ICCSIT), 2010 3<sup>rd</sup> IEEE International Conference on, pp. 539-542, 2010, ISBN 978-1-4244-5537-9, DOI: 10.1109/ICCSIT.2010.5563610
- [19] Ohm, D. Y.: Dynamic Model of PM Synchronous Motors, Available on <[www.drivetechnic.com/articles/IM97PM\\_Rev1forPDF.pdf](http://www.drivetechnic.com/articles/IM97PM_Rev1forPDF.pdf)> [accessed 11.1.2012]
- [20] Pillay, P. – Krishan, R.: Modeling of Permanent Magnet Motor Drives, In: IEEE Transactions on industrial electronics, Vol. 35, No. 4, November 1988, pp. 537-541, ISSN 0278-0046, DOI 10.1109/41.9176

- [21] Perera, P. D. C. – Blaabjerg, F. – Thogersen, P.: A Sensorless Stable V/f Control Method for Permanent-Magnet Synchronous Motor Drives, In: IEEE Transactions on Industry Applications, Vol. 39, pp. 783-791, May-Jun 2003
- [22] Novak, M. - Novak, J. - Chysky, J.: Experimental Verification of High-Speed Permanent Magnet Synchronous Motor Model, In: Proceedings of Electrical Machines (ICEM) 2012, 20<sup>th</sup> International Conference on , Vol., No., pp. 2435-2440, 2-5 Sept. 2012, doi: 10.1109/ICEIMach.2012.635022
- [23] Zwysig, C. – Round, S. D. – Kolar, J. W.: Analytical and Experimental Investigation of a Low Torque, Ultra-High Speed Drive System, In.: Proceedings of the Industry Applications Conference, 2006, 41<sup>st</sup> IAS Annual Meeting. Conference Record of the 2006 IEEE, pp. 1507-1513, ISBN 1-4244-0364-2, DOI: 10.1109/IAS.2006.256729
- [24] Venkatachalam, K. – Sullivan, Ch. R. – Abdallah, T. – Tacca, H.: Accurate Prediction of Ferrite Core Loss with Nonsinusoidal Waveforms Using Only Steinmetz Parameters, In: Proceedings of IEEE Workshop on Computers in Power Electronics, 2002, pp. 36-41, ISBN 0-7803-7554-8, DOI: 10.1109/CIPE.2002.1196712
- [25] Chen, Y. – Pillay, P.: An Improved Formula for Lamination Core Loss Calculations in Machines Operating with High Frequency and High Flux Density Excitation, In.: Conference Record of the Industry Applications Conference, 2002, 37<sup>th</sup> IAS Annual Meeting., pp. 759-766, Vol. 2, ISBN 0-7803-7420-7, DOI: 10.1109/IAS.2002.1042645
- [26] Flah, A. – Sbita, L, " An Adaptive High Speed PMSM Control for Electrical Vehicle Application”, In: Journal of Electrical Engineering JEE, Vol. 12, No. 3, 2012
- [27] Verghese, G. C. – Lang, J. H. – Casey, L. F.: Analysis of Instability of Electrical Machines, In: IEEE Transactions on Industrial Applications, Vol. IA-22, No. 5, pp. 853-864, 1986
- [28] Mellor, P. H. – Al-Tae, M. A. – Binnks, K. J.: Open Loop Stability Characteristics of Synchronous Drive Incorporating High Field Permanent Magnet Motor, In: IEE Proc. Electr. Power Applicat, Vol. 138, No. 4, pp. 175-184, 1991
- [29] Zhao, L. – Ham, C. H. – Zheng, L. – Wu, T. – Sundaram, K. – Kapat, J. – Chow, L.: A Highly Efficient 200 000 RPM Permanent Magnet Motor System, In: IEEE Transactions on Magnetics, Vol. 43, Issue 6, pp. 2528-2530, 2007
- [30] Zhao, L. – Ham, C. H. – Wu, T. X. – Zheng, L. – Sundaram, K. B. – Kapat, J. – Chow, L.: Design of Optimal Digital Controller for Stable Super-High-Speed Permanent-Magnet Synchronous Motor, IEE Proc. Electr. Power Appl., Vol. 153, No. 2, March 2006, pp. 213-218

- [31] Borisavljevic, A. – Brands, M. – Lomonova, E.: Vector Control of Very-High-Speed PM Machines, In: Proceedings of the International Conference of Electrical Machines (ICEM 2012) September 2-5 2012, Marseille, France, pp. 2460-2466, Piscataway: IEEE Service Center
- [32] Ham, C. – Zhao, L. – Zheng, L. – Wu, T. – Sundaram, K. – Kapat, J. – Chow, L.: Development of an Ultra High-Speed Permanent Magnet Synchronous Motor (PMSM) System for a Liquid Hydrogen Cryocooler, In: Proceedings of the International Conference on Electrical Engineering (ICEE), 2006, Available on < <http://www.icee-con.org/papers/2006/pdf/PS2-EM-01.pdf> >, [accessed 30.9.2012]
- [33] Liu, K. – Zhang, Q.: Comparison of Two Novel MRAS-based Strategies for Identifying Parameters in Permanent Magnet Synchronous Motors, In: International journal of automation and computing, pp. 516-524 (2010)
- [34] Vyhlídal, T. – Zitek, P.: Mapping-based Algorithm for Large-Scale Computation of Quasi-Polynomial Zeros. In: IEEE Transactions on Automatic Control. 2009, Vol. 54, No. 1, pp. 171-177, ISSN 0018-9286
- [35] Vyhlídal, T. - Zitek, P.: Quasipolynomial Mapping-based Rootfinder for Analysis of Time Delay Systems, In: Time Delay Systems 2003 – A Proceedings volume from the 4<sup>th</sup> IFAC workshop, Rocquencourt, France, Elsevier: Oxford, pp. 227-232
- [36] Michiels, W. – Vyhlídal, T.: An Eigenvalue-based Approach for the Stabilization of Linear Time-Delay Systems of Neutral Type. In: Automatica. 2005, Vol. 41, No. 6, pp. 991-998, ISSN 0005-1098